

Compact Optically Pumped High Power Midwave IR Lasers

**Greg Martinez
Dr. Yong-Hang Zhang
Dr. Shane Johnson
Peter Terek**

**Optolocity LLC
7259 E. Cortez Rd.
Scottsdale, AZ 85260**

August 2001

Final Report

APPROVED FOR PUBLIC RELEASE; DISTRIBUTION IS UNLIMITED

20020213 109



**AIR FORCE RESEARCH LABORATORY
Directed Energy Directorate
3550 Aberdeen Ave SE
AIR FORCE MATERIEL COMMAND
KIRTLAND AIR FORCE BASE, NM 87117-5776**

Using Government drawings, specifications, or other data included in this document for any purpose other than Government procurement does not in any way obligate the U.S. Government. The fact that the Government formulated or supplied the drawings, specifications, or other data, does not license the holder or any other person or corporation; or convey any rights or permission to manufacture, use, or sell any patented invention that may relate to them.

This report has been reviewed by the Public Affairs Office and is releasable to the National Technical Information Service (NTIS). At NTIS, it will be available to the general public, including foreign nationals.

If you change your address, wish to be removed from this mailing list, or your organization no longer employs the addressee, please notify AFRL/DELS, 3550 Aberdeen Ave SE, Kirtland AFB, NM 87117-5776.

Do not return copies of this report unless contractual obligations or notice on a specific document requires its return.

This report has been approved for publication.


CHARLES E. MOELLER, DR-III
Project Manager


SYLVIA DORATO, DR-III
Chief, Tactical Laser Branch

FOR THE COMMANDER


R. EARL GOOD, SES
Director, Directed Energy

REPORT DOCUMENTATION PAGE				<i>Form Approved</i> OMB No. 0704-0188	
Public reporting burden for this collection of information is estimated to average 1 hour per response, including the time for reviewing instructions, searching existing data sources, gathering and maintaining the data needed, and completing and reviewing this collection of information. Send comments regarding this burden estimate or any other aspect of this collection of information, including suggestions for reducing this burden to Department of Defense, Washington Headquarters Services, Directorate for Information Operations and Reports (0704-0188), 1215 Jefferson Davis Highway, Suite 1204, Arlington, VA 22202-4302. Respondents should be aware that notwithstanding any other provision of law, no person shall be subject to any penalty for failing to comply with a collection of information if it does not display a currently valid OMB control number. PLEASE DO NOT RETURN YOUR FORM TO THE ABOVE ADDRESS.					
1. REPORT DATE (DD-MM-YYYY) 10-08-2001		2. REPORT TYPE Final Report		3. DATES COVERED (From - To) 01-05-2000 – 15-07-2001	
4. TITLE AND SUBTITLE Compact Optically Pumped High Power Midwave IR Lasers				5a. CONTRACT NUMBER F29601-00-C-0103	
				5b. GRANT NUMBER	
				5c. PROGRAM ELEMENT NUMBER 65502F	
6. AUTHOR(S) Greg Martinez Dr. Yong-Hang Zhang Dr. Shane Johnson Peter Terek				5d. PROJECT NUMBER 3005	
				5e. TASK NUMBER DO	
				5f. WORK UNIT NUMBER EF	
7. PERFORMING ORGANIZATION NAME(S) AND ADDRESS(ES) Optolocity LLC 7259 E. Cortez Rd. Scottsdale, AZ 85260				8. PERFORMING ORGANIZATION REPORT NUMBER N/A	
9. SPONSORING / MONITORING AGENCY NAME(S) AND ADDRESS(ES) AFRL/DELS 3550 Aberdeen Ave SE Kirtland AFB NM 87117-5776				10. SPONSOR/MONITOR'S ACRONYM(S)	
				11. SPONSOR/MONITOR'S REPORT NUMBER(S) AFRL-DE-TR-2001-1067	
12. DISTRIBUTION / AVAILABILITY STATEMENT Approved for public release; distribution is unlimited					
13. SUPPLEMENTARY NOTES					
14. ABSTRACT We have proposed a novel packaging scheme for high-power optically pumped mid-wave infrared lasers. The proposed device module does not require optics for alignment and is very compact in size. The module is made from copper and allows the pump laser to be moved relative to the mid-wave infrared laser by adjusting set-screws. Room temperature Fourier transform infrared spectroscopy measurements have been performed to measure the electroluminescence spectrum of the optically pumped mid-wave infrared laser which emits at 3.08 μm at room temperature. The best results were obtained at 77 K where we observe weak electroluminescence at approximately 2.7 μm . The optical pumping wavelength is 0.809 μm with a current of 10 A and 6 W of optical power.					
15. SUBJECT TERMS Optically pumped laser design, compact optically pumped semiconductor laser					
16. SECURITY CLASSIFICATION OF:			17. LIMITATION OF ABSTRACT Unlimited	18. NUMBER OF PAGES 22	19a. NAME OF RESPONSIBLE PERSON Charles Moeller
a. REPORT Unclassified	b. ABSTRACT Unclassified	c. THIS PAGE Unclassified			19b. TELEPHONE NUMBER (include area code) (505) 846-7033

TABLE OF CONTENTS

	Page
I. EXECUTIVE SUMMARY.....	1
II. PROJECT SUMMARY.....	2
III. TECHNICAL REPORT.....	3
Task 1.1 Fabricate 980 nm laser bars using commercial or ASU MBE grown wafers.....	3
Task 1.2 Design the preliminary package structure.....	7
Task 1.3 Demonstrate the package module with proper alignment of the pumping laser and the mid-wave infrared laser on a bench in the lab.....	9
Task 1.4 Assemble a demonstration model.....	10
Task 2.1 Theoretical analysis of the InAs substrate-based InGaAsSb bandgaps as function of compositions.....	10
Task 2.2 Design overall device structure, including calculating the confinement factor, etc.....	14
Task 2.3 Fabricate 980 nm laser bars using commercial or ASU MBE grown wafers...	14
Task 2.4 Device fabrication and characterization.....	14
IV. SUMMARY.....	14
V. LESSONS LEARNED.....	14
VI. PROPOSAL FOR FUTURE WORK.....	15
VII. REFERENCES.....	15

LIST OF FIGURES

Figure 1.....	Page 6
Figure 2.....	6
Figure 3.....	7
Figure 4.....	8
Figure 5.....	8
Figure 6.....	8
Figure 7.....	9
Figure 8.....	13
Figure 9.....	13

I. Executive Summary

In the final report period, we discuss the results obtained during this project. The main technical effort for the Phase I program focused on demonstrating an optically pumped long wavelength laser using a novel packaging scheme that does not use any optics for the alignment. Without aligning optics, the package is extremely compact and robust. In this program, we used a 980nm or similar pump laser to pump a mid-wave infrared (MWIR) laser. By doing so, the heat generated by the injected-electron thermal relaxation in the MWIR laser is minimized. The active region of the MWIR laser is then less heated. Since MWIR lasers are very sensitive to the active region temperature, such an arrangement will result in a dramatic improvement of the device performance.

Tasks for Phase I:

Approach 1:

- Task 1.1 Fabricate 980 nm laser bars using commercial or Arizona State University molecular beam epitaxy (MBE) grown wafers. (Finished)
- Task 1.2 Design the preliminary package structure. (Finished)
- Task 1.3 Demonstrate the package module with proper alignment of the pumping laser and the MWIR laser on a bench in the lab. (Finished)
- Task 1.4 Assemble a demonstration module. (Finished)

Approach 2:

- Task 2.1 Theoretical analysis of the InAs substrate-based InGaAsSb bandgaps as function of compositions. (Finished)
- Task 2.2 Design overall devices structure, including calculating the confinement factor etc. (Finished)
- Task 2.3 MBE growth of 2 laser structures and 6 calibration runs. (Finished)
- Task 2.4 Device fabrication and characterization. (Finished)

II. Project Summary

This Phase I program provides an opportunity for Optolocity to demonstrate a prototype heatsink module. In particular, the goal of this project is to design and fabricate a compact optically pumped high power MWIR laser. The highest power output of semiconductor MWIR lasers demonstrated so far is from optically pumped lasers. The optical pumping approach dramatically reduces the heat generation by overcoming the quantum defect in the MWIR lasers. Although the overall power efficiency, including that of the pumping laser, will not increase, this approach still has its technical merit because the heat management for the pumping laser is much easier to deal with than that for MWIR lasers. The shorter wavelength pumping lasers have much less temperature sensitivity compared with MWIR lasers. However, one noticeable drawback for previous optical pumping MWIR laser devices is its bulky optical packaging. The present approach proposes an innovative simple packaging scheme that will provide a very compact and robust design for optically pumped high-power MWIR lasers without the need for using optics for the alignment.

Although the research on MWIR lasers has made substantial progress in the past years, there are still several key issues that need to be addressed. Several groups have demonstrated that the threshold current density of MWIR lasers at low temperature ($\sim 10\text{K}$) can be extremely low, 3 A/cm^2 for $3.4\text{ }\mu\text{m}$ InAs/InAsSb SL lasers at 20K and 9 A/cm^2 for $3\text{ }\mu\text{m}$ InGaAsSb double heterostructure (DH) laser at 30K . However, the typical values of T_0 for these devices are only $50\text{-}20\text{K}$, decreasing for longer wavelength devices.

Low power efficiency of MWIR lasers has also been a long-standing issue. It is partially attributed to the "quantum defect" that describes energy efficiency loss due to the thermal relaxation of hot electrons injected into the active region from wide bandgap cladding materials. The larger the difference between the bandgaps of the active region and the cladding layer is, the larger the quantum defect. Optical pumping provides a route to bypass this issue, since the pumping light can have much lower energy than the bandgap of the cladding layers.

Optically pumped MWIR lasers have some unique features to overcome these problems. By using a 980 nm laser as a pump laser, the heat generated by the injected-electron thermal relaxation will be minimized. The active region of the laser is then less heated. Since the MWIR lasers are very sensitive to the active region temperature, such an arrangement will result in a dramatic improvement of the device performance. The heat generated in the 980nm pump lasers can be much easily handled. Due to the mature materials and technology for 980nm lasers, the overall module performance will be improved compared with electrically injected MWIR lasers. This method has experimentally demonstrated high power outputs. However, the conventional approaches require some optics to align the output light from the pump laser and to focus it on to the MWIR laser. Such a setup is not compact and a lot of lights from the pump laser will loss due to the limited size of the optics.

Due to the lack of qualified students and researchers with United States citizenship at ASU, the original plan to grow the MWIR laser wafers at ASU was modified. Instead, we decided to use a commercially available pump laser and contacted several vendors to search for a suitable pump laser. The vendors we contacted include Optopower, SDL, and IMC Laser.

We also performed some preliminary calculations to determine the distance between the pump laser and MWIR laser. The distance depends on the pump laser beam size and the threshold power density of the MWIR laser.

In the Second report, we designed and fabricated a heatsink module. The heatsink is made of copper and consists of three pieces that allow the adjustment of the pump laser and the MWIR laser in two directions. We also purchased a 2 W pump laser from IMC Laser.

In the Third report, we received the pump laser from IMC Laser. We also obtained a 3.1 μm MWIR laser from Naval Research Labs. Calculations were also done to determine the pumping density needed to get the MWIR laser to lase.

In the Fourth report, we began doing room temperature Fourier transform infrared spectroscopy (FTIR) measurements with the laser package. We tried using a lock-in amplifier, but the results were not useful because our current pulse generator only has a duty cycle of 10%, so we were not able to obtain enough pump power. Because of this limitation, we began setting up the measurement with a direct current (DC) current source. This should increase the pumping power by approximately 50 \times . We also worked on setting up the optics better so we can focus the maximum amount of light into the FTIR system.

III. Technical Report

We have demonstrated a laser packaging module to optically pump a MWIR laser using a 980 nm or similar pump laser. The module is compact and can work without using any optics. A detailed report on the tasks in this program are as follows:

Task 1.1 Fabricate 980 nm laser bars using commercial or ASU MBE grown wafers

First, we consider the estimated power needed to pump a 3 μm Sb-based MWIR laser using a commercially available laser in the wavelength range of 808-980 nm. The published data on absorbed threshold power or the power density for optically pumped MWIR lasers vary considerably, from mW to kW, depending on the focusing conditions and temperature. The power needed will also depend on the beam size and the structure of the MWIR laser (cladding layers, etc.). We take $1\text{kW}/\text{cm}^2$ as the absorbed threshold power density and choose a laser stripe size of $1\text{mm} \times 100\mu\text{m}$, (i.e., the cavity length 1 mm and the pumped stripe width of 100 μm). In this case, the absorbed threshold power will be 1 W. We can easily select a pumping laser at 980 nm with a power output ranging between 1 to 5 W.

For our module, we examined several different vendors who provide lasers that emit around 808-980 nm at 1-5 W, including SDL, Optopower, Semiconductor Laser International, IMC Laser, and High Power Devices Inc. Below are the specifications for a typical 2 W 980 nm laser.

Parameters	Min.	Typical	Max.	Unit
Power	2		5	W
Threshold current	240	300	360	mA
Operating current	2000	2400	3000	mA
Operating temperature	25			C
Emitter size	200x1			μm
Beam Divergence (vertical)	35	40	45	degree
Beam Divergence (lateral)	8	8	8	degree
Voltage	1.6	1.8	2.0	V
Slope efficiency	0.7	0.9	1.1	W/A
Wavelength tolerance	3.0	5.0		+ - nm
Packaging	c-mount or HPC mount			

The long wavelength laser we obtained was grown by Naval Research Labs and has a wavelength of $3.08 \mu\text{m}$ at room temperature. The specifications (Sample A) of this MWIR laser can be found in a paper by Bewley, *et al.*, where they used a pulsed $2.1 \mu\text{m}$ Q-switched Ho:yttrium-aluminum-garnet (YAG) laser to optically pump the MWIR laser [1]. Sample A has an all binary active region that is a 50-period InAs/GaSb/InAs/AlSb ($18 \text{ \AA}/25 \text{ \AA}/18 \text{ \AA}/35 \text{ \AA}$) W multiple quantum well, which is surrounded by a $2 \mu\text{m}$ thick $\text{Al}_{0.9}\text{Ga}_{0.1}\text{As}_{0.07}\text{Sb}_{0.93}$ top and bottom optical cladding layer. The total thickness of the active region is approximately 3050 \AA (ignoring the contribution from the AlSb layer, which should be insignificant). They report that Sample A has a full width at half maximum (FWHM)= 20 nm and that the wavelength varied linearly from $2.80 \mu\text{m}$ (3571 cm^{-2}) at 100 K to $3.18 \mu\text{m}$ at 350 K . From Fig. 2 in the Bewley paper, we would need a threshold current density of around 40 kW/cm^2 at room temperature, but only 1.5 kW/cm^2 at 77 K to get the sample to lase. To achieve lasing at room temperature, the pump laser will need to be about 0.2 mm above the MWIR laser. With our pump laser 0.2 mm from the MWIR laser, we can focus to a spot size of around $0.04 \text{ mm} \times 0.15 \text{ mm}$ and have a peak pump intensity of about 41 kW/cm^2 . The peak output power of the MWIR laser is about 500 mW per facet if the peak pump intensity is 200 kW/cm^2 (Fig. 1 in Bewley's paper). If the pump intensity is 41 kW/cm^2 , then the MWIR output power should be around 120 mW .

For a laser beam divergency of $8^\circ \times 40^\circ$, we calculated the Beam size vs. Distance as shown in Table 1. We can see from the calculations that when the distance between the pump laser and the MWIR laser changes from 0.5 mm to 10 mm , the beam width along vertical direction of the pumping laser will change from 0.36 mm to 7.3 mm , while that along lateral direction changes from $35 \mu\text{m}$ to $700 \mu\text{m}$. This range will be enough to pump various MWIR lasers with different dimensions. At $X=2.75 \text{ mm}$, we obtain the beam size about $2 \text{ mm} \times 200 \mu\text{m}$, which is very suitable and practical to pump our MWIR lasers. Also included in the table are the power density values for various pump laser powers. For Sample A, we would need to pump with more than 4 W at 77 K to get the MWIR laser to work and have a sample size of around $1 \text{ mm} \times 2 \text{ mm}$. The distance between the two lasers would be around 1 to 2 mm .

Table 1: Beam size vs. Distance assuming a beam divergency of $8^\circ \times 40^\circ$

Distance between two lasers X (mm)	Beam size (Long axis)	Beam size (Short axis)	Power=2W kW/cm ²	Power=4 W kW/cm ²	Power=8 W kW/cm ²
X = 0.5 mm	0.36 mm	35 μ m	16	32	64
X = 2.75 mm	2 mm	200 μ m	0.5	1	2
X = 5 mm	3.6 mm	350 μ m	0.16	0.32	0.64
X = 10 mm	7.3 mm	700 μ m	0.040	0.080	0.160

For this project, we obtained three different pump lasers. The specifications for each laser are listed in Table 2. The first pump laser was obtained from IMC Laser. This laser was mounted directly onto our heatsink and consists of a single emitter. The maximum laser current was 2.4 A. The lifetime of the laser above this current is unknown, so they recommended that we operate in a range around 2.0 A. The laser power is not as high as we had hoped. The second laser was obtained from Optopower and also consists of a single emitter. This laser operates at 980 nm and puts out 2 W.

To obtain even higher pumping power, laser arrays can be used to pump the MWIR lasers, so we also obtained a laser array from Optopower. This laser consists of an array with seven emitters. Each emitter is 150 μ m wide and the array has a period of 650 μ m. The beam divergency is 40° by 8° . The light intensity-current-voltage (LIV) curve is shown in Fig. 1. The recommended maximum power is around 15 W, which is more than enough for our application. We estimate that we need around 40 kW/cm² at room temperature and around 1 kW/cm² at 77 K. We should be able to obtain this power density at around 8 W at 77 K. The electroluminescence curve for the laser array is shown in Fig. 2. The array emits at around 809 nm and has a FWHM of around 20 nm.

Table 2: Specifications of the pump laser purchased from IMC Laser

Parameters	IMC Laser	Optopower	Array	Units
Wavelength	980	980	809	nm
Power	2	2	15	W
Threshold current	500		4.34	mA
Operating current	2500		10	mA
Operating temperature	300		300	K
Emitter size	150 \times 1		150 \times 7	μ m
Beam Divergence (vertical)	35		40	degree
Beam Divergence (lateral)	10		8	degree
Voltage	1.6		1.8	V
Slope efficiency	0.7			W/A
Wavelength tolerance	3.0			\pm nm

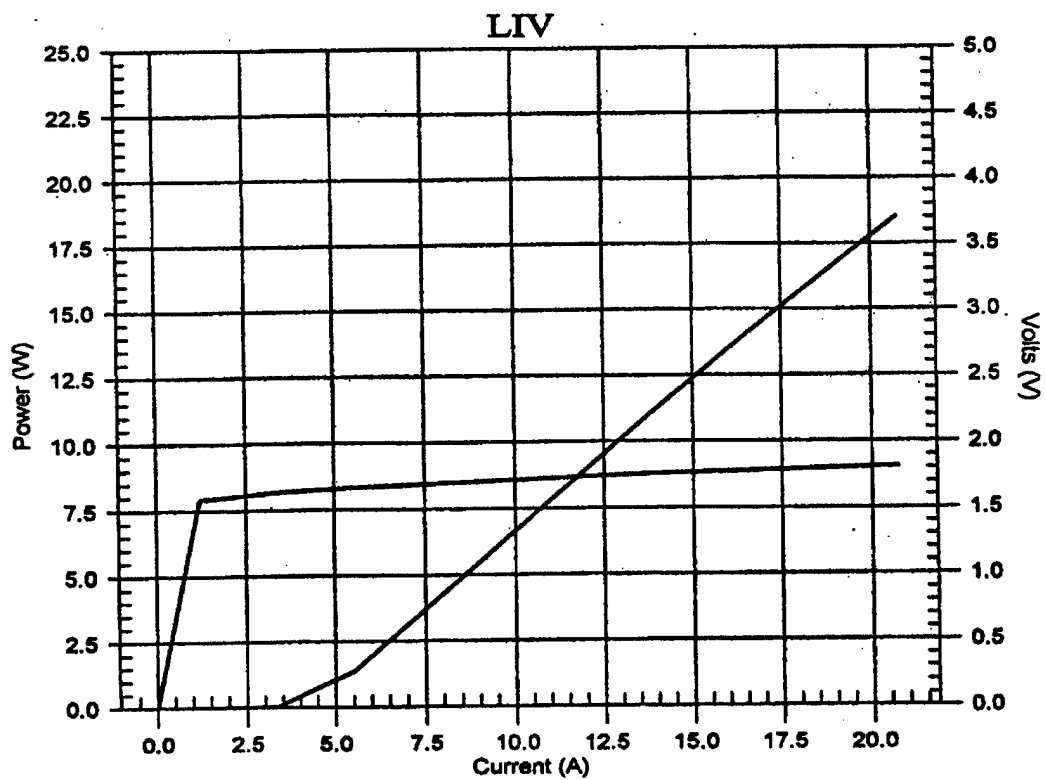


Fig. 1. The LIV curve for the laser array obtained from Optopower. This laser array consists of seven emitters.

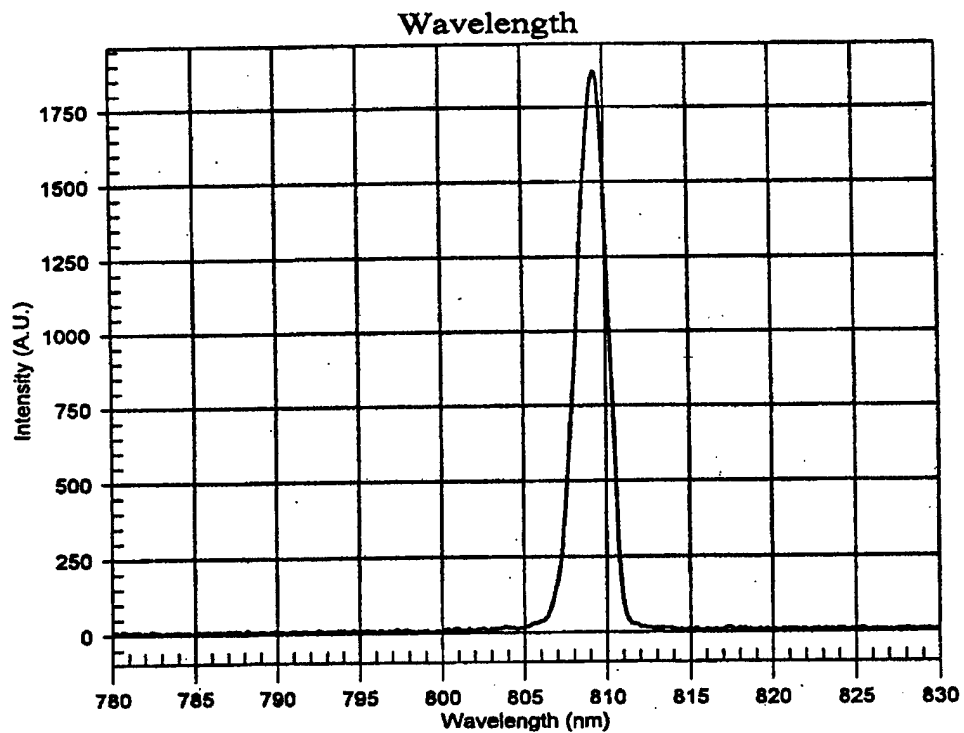


Fig. 2. The electroluminescence spectra of the laser array obtained from Optopower.

Task 1.2 Design the preliminary package structure.

Several heatsink designs were fabricated because the pump lasers we obtained from Optopower were already mounted on their own heatsink. The first heatsink structure is shown in Fig. 3. We were able to use this design for the first module because IMC Laser was willing to mount their laser onto our heatsink. The lasers obtained from Optopower were already mounted onto heatsinks, so we had to design around them.

The heatsinks are all made of copper and the three pieces are held together using 0-80 screws. The lasers sit on removable pieces to facilitate changing either laser and are held together by a frame, as indicated in Fig 1. The 0-80 setscrews are also used to adjust the position of the pump laser and the optically pumped laser in the x - and z -directions. This allows the pump laser to be focused onto the optically pumped laser without having to use lenses or other optics. The use of optics to align the output beam from the pump laser is not very compact and is inefficient because of optical losses. In the x -direction, the two outside screws act as legs, while the center screw is used to clamp the piece to the frame. In the z -direction, we used four screws for the legs and added one center screw (not shown) to clamp this piece to the frame.

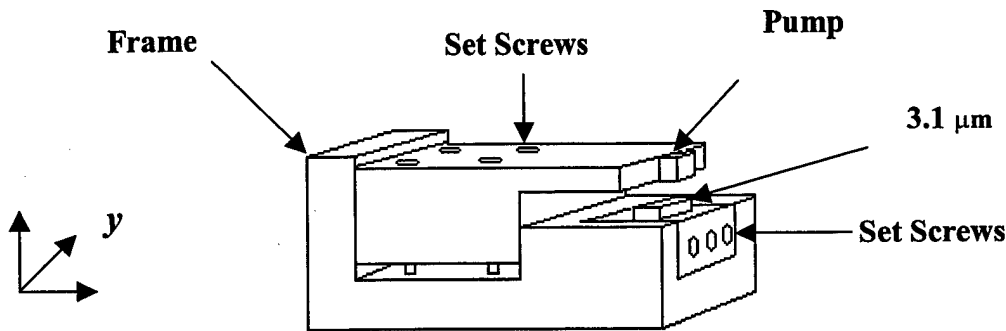


Fig. 3. The copper heatsink designed to allow the position of the pump laser to be adjusted relative to the optically pumped laser.

The range of motion of the pieces is limited by the length of the setscrews. To increase the range, we had the holes for the screws widened so that the heads are embedded. The range of motion is about 2 mm, but the focusing length of the pump laser will depend on the thickness of the optically pumped laser. The focusing distance of these two lasers will depend on the threshold power density of our MWIR laser. The entire package is 30×15×15 mm, but could probably be made smaller if desired.

One concern with this design is that the optically pumped laser is mounted on a piece of copper that is too small to adequately remove the heat. It is important to dissipate heat from the optically pumped laser because MWIR lasers are very sensitive to the active region temperature. The temperature sensitivity issue is the main drawback to electrically modulating MWIR lasers. The next heatsink design addresses this concern by increasing the size of this copper piece. Also, the optically pumped laser needs to be closer to an edge so that the laser beam will not experience any interference effects. Fig. 4 shows the second heatsink design that will be fabricated. As can be seen, the copper piece holding the optically pumped laser has been made

significantly larger and a notch in the frame has been added so that this laser is closer to an edge to minimize any interference effects.

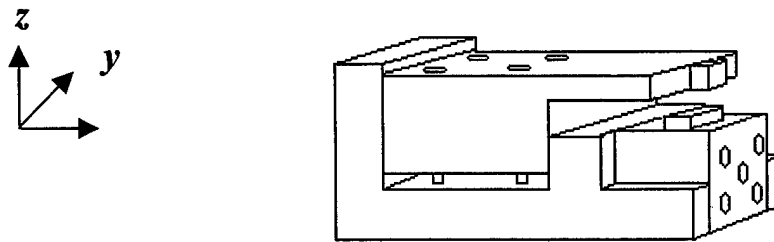


Fig. 4 The copper heatsink redesigned to allow better heat dissipation from the optically pumped laser and to minimize interference effects.

Another heatsink design we fabricated is illustrated in Fig. 5. This heatsink allows us to use a laser already mounted onto a C mounted heatsink. The C mount heatsink is held in place with a 0-80 screw.

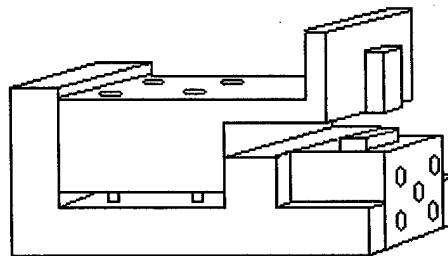


Fig. 5 The copper heatsink redesigned to allow a laser already mounted on a C mount heatsink to be integrated into the module.

The final heatsink design is illustrated in Fig. 6. We fabricated this module so that it can be used both with and without a lens. The lens is held with a copper holder (not shown). We designed a system where we can adjust the focusing mirror with some by sliding the copper lens holder through a groove. This allows us to change the focal point of the pump laser.

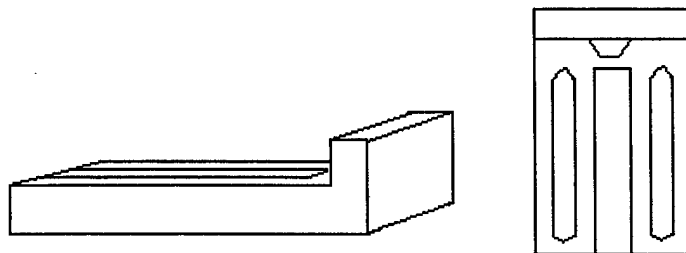


Fig. 6 The final copper heatsink design to allow a laser already mounted on a Cs heatsink to be integrated into the module. The view on the left is from the side and the view on the right is from the top.

Task 1.3 Demonstrate the package module with proper alignment of the pumping laser and the MWIR laser on a bench in the lab.

The laser modules discussed in Task 1.2 above were tested with the MWIR laser. We used a Xantrex XFR 40-30 DC power supply for the pump laser. Using a DC current source should increase the pumping power by about 50 \times . The most useful results we obtained were with the Cs mounted diode array where we could optically pump with more than 4 W. The results are shown in Fig. 7. This measurement was done at 77 K with the heatsink mounted in a silver coated glass dewar. The current is 10 A and the pump power is about 6 W. The pump laser was approximately 1 mm from the MWIR laser bar and was not focused. The MWIR laser bar is approximately 1 mm \times 2 mm. To finish assembling the module, we lapped the MWIR laser to 200 μ m then cut it into laser bars. The laser bars are about 750 μ m wide. The MWIR laser bars were then mounted onto the heatsink by using silver paste.

The resulting FTIR spectra is illustrated in Fig. 7. The MWIR laser emits at around 2.7 μ m. This result is expected because the Bewley paper reported a peak at 2.80 μ m at 100 K. The signal is relatively weak, but this is probably due to the fact that we are using a 809 nm laser array. We would obtain a significantly stronger signal with a longer wavelength array, such as 980 nm. However, this result shows that we are able to align the pump laser with the MWIR laser. Unfortunately, the FWHM of this peak is approximately 80 nm, which indicates that the MWIR laser is not lasing.

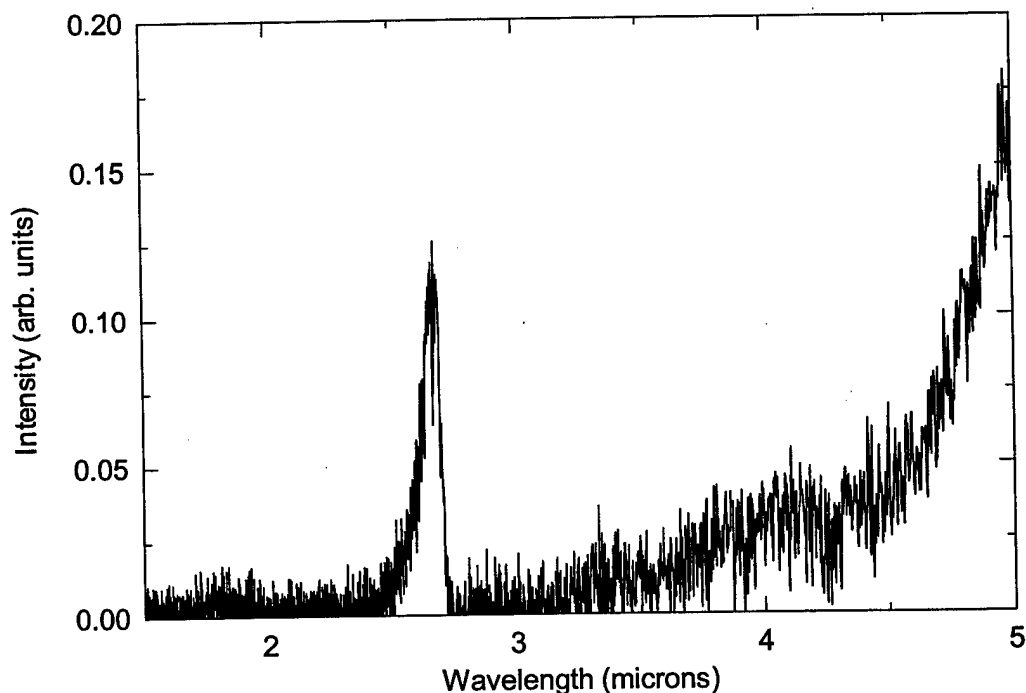


Fig. 7 Low temperature spectra of the MWIR laser pumped with the 809 nm laser array. The measurement was performed at 77 K with the FTIR system. The laser array current was about 10 A and 6 W. The FWHM of this peak is approximately 80 nm.

Task 1.4 Assemble a demonstration module.

The demonstration module consists of the Cs mounted laser array heatsink. We obtained the best results with this laser array because we could obtain the necessary optical pump power. The laser array was already mounted on a Cs heatsink, so we designed our module around this. This design is shown in Fig. 6 above. We were only able to obtain luminescence from the MWIR laser at 77 K when pumping with the laser array at 6 A and 10 W. This result indicates that we are able to align the two lasers with our module and obtain a signal. There are several reasons as to why the MWIR laser was not lasing. Firstly, the alignment of the two lasers probably was not optimized. Given their small dimensions it is difficult to adjust the lasers relative to one another. Secondly, we only had a small piece of the MWIR laser to work with and it was difficult to achieve high quality cleaved mirror facets. A commercially cleaved sample would be highly desirable so we know that if we do not get a signal, then it is due to the alignment and not because the MWIR laser is not cleaved properly.

Task 2.1 Theoretical analysis of the InAs substrate-based InGaAsSb bandgaps as function of compositions.

III-V compound semiconductor material systems used for 2 μm lasers include InGaAs/GaInAsP/InP quantum well structures and InGaAsSb and InAsPSb quaternary alloys lattice matched to either InAs or GaSb substrate. The first system uses InGaAs as the quantum well and InGaAsP as the barrier and the wave-guiding layers. The InP is used for the cladding layers. Using strain compensation, the wavelength can be extended beyond 2 μm . But it will be very difficult to extend the wavelength to longer than 2.3 μm .

GaInAsSb quaternary material, on the other hand, is broadly used for the fabrication of MWIR lasers and detectors. Using GaSb or InAs substrate, the wavelength can cover from 1.72 μm (pure GaSb, $E_g = 0.726 \text{ eV}$) to 4.2 μm (corresponding to $\text{InAs}_{0.9}\text{Sb}_{0.1}$, $E_g = 0.296 \text{ eV}$). Due to the small lattice constant difference between InAs ($a = 6.0584\text{\AA}$) and GaSb ($a = 6.0959\text{\AA}$), the lattice-matched compositions for this quaternary material are very similar for both substrates. In this program, we focus our attention on InGaAsSb quaternary materials grown on GaSb substrates. Here, we give a theoretical analysis of GaSb-based InGaAsSb band gap as function of compositions.

The key advantage to use quaternary material is the fact that we can easily choose composition to obtain the desired emission wavelength and the lattice-matched lattice constant. In double heterostructure MWIR laser structures, the composition dependent lattice constant and wavelength of InGaAsSb quaternary layers can be calculated using an interpolation scheme. Therefore, the band gap and the lattice constant of GaInAsSb quaternary material can be derived from the parameters of the four binaries GaAs, GaSb, InAs, and InSb, as well as their ternaries GaInAs, GaInSb, GaAsSb, and InAsSb. The lattice constant is assumed to obey the well-known Vegard's law, i.e., the $\text{In}_x\text{Ga}_{1-x}\text{As}_y\text{Sb}_{1-y}$ lattice constant can be expressed as:

$$a(\text{In}_x\text{Ga}_{1-x}\text{As}_y\text{Sb}_{1-y}) = xy a(\text{InSb}) + x(1-y)a(\text{InAs}) + (1-x)y a(\text{GaSb}) + (1-x)(1-y) a(\text{GaAs}) \quad (1)$$

Using the lattice constants of the four binaries, the lattice-match condition for $\text{In}_x\text{Ga}_{1-x}\text{As}_{1-y}\text{Sb}_y$ /GaSb system can be easily derived as:

$$y = (1-0.92x)/(1-0.07x) \quad (0 < x < 1).$$

For determining the band gap of the quaternary alloy, based on the equation proposed by Moon et al., the energy band gap can be expressed as

$$E_g(x, y) = x E(\text{GaAsSb}) + (1-x) E(\text{InAsSb}) - \Delta, \quad (2)$$

where Δ represents the bowing parameter term which is determined by the compositions and the four ternary bowing parameters:

$$\Delta = x(1-x) [(1-y) C(\text{InGaSb}) + y C(\text{InGaAs})] + y(1-y) [x C(\text{InAsSb}) + (1-x) C(\text{GaAsSb})],$$

where $C(\text{ijk})$ is the bowing parameter of a ternary material.

If equation (1) equals the lattice constant of GaSb and one can solve this equation together with equation (2), then, the exact quaternary compositions at desired emission wavelength can be obtained. We have calculated the exact compositions for each emission wavelength in the range of 1.8-3.0 μm (see table below). All compositions are closely lattice matched to GaSb substrate. It is worthy to mention that H.K. Choi and S.J. Eglash in Lincoln Laboratory demonstrated room temperature CW operation of InGaAsSb/AlGaAsSb diode laser at 2.2 μm wavelength, the In and Sb compositions they reported are 0.16 and 0.86, respectively, indicating that the theoretical calculation of the wavelength dependent compositions is useful in device design [2]. Constant energy contours for the $\text{In}_x\text{Ga}_{1-x}\text{As}_{1-y}\text{Sb}_y$ material system are shown in Fig. 8. Constant lattice constant contours for the $\text{In}_x\text{Ga}_{1-x}\text{As}_{1-y}\text{Sb}_y$ material system are shown in Fig 9.

Table 3: Calculated wavelength (bandgap) as function of alloy compositions.

Wavelength (μm)	Energy (eV)	Solid compositions			
		In	Ga	As	Sb
1.8	0.689	0.0012	0.9988	0.0010	0.9990
1.9	0.653	0.0437	0.9563	0.0373	0.9627
2.0	0.62	0.0841	0.9159	0.0720	0.9280
2.1	0.591	0.1215	0.8785	0.1043	0.8957
2.2	0.56	0.1616	0.8384	0.1391	0.8609
2.3	0.539	0.1903	0.8097	0.1641	0.8359
2.4	0.52	0.2170	0.7830	0.1875	0.8125
2.5	0.496	0.2520	0.7480	0.2183	0.7817
2.6	0.477	0.2809	0.7191	0.2439	0.7561
2.7	0.46	0.3078	0.6922	0.2677	0.7323
2.8	0.443	0.3360	0.6640	0.2929	0.7071
2.9	0.428	0.3621	0.6379	0.3162	0.6838
3.0	0.413	0.3883	0.6117	0.3397	0.6603

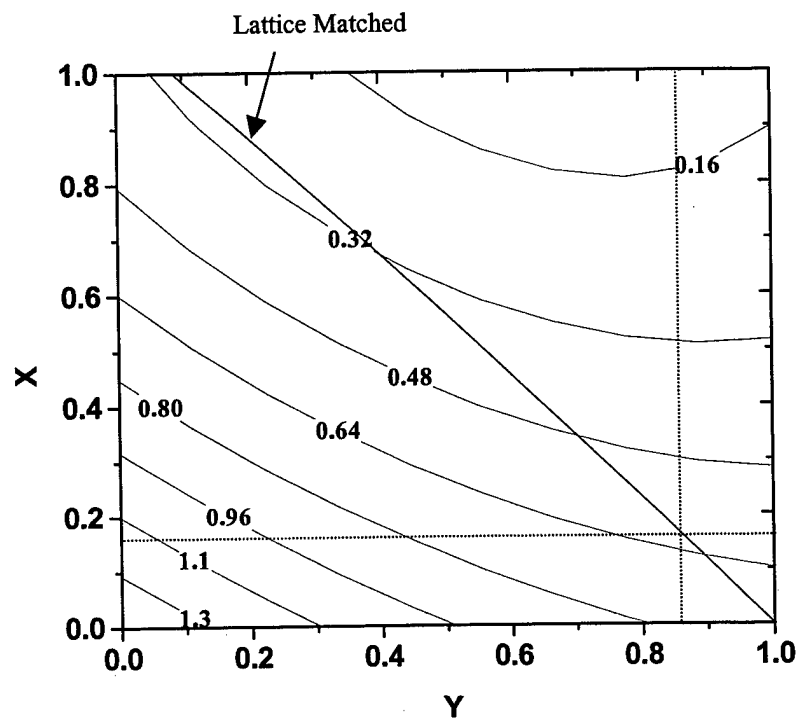


Fig. 8 Constant energy contours for the $\text{In}_x\text{Ga}_{1-x}\text{As}_{1-y}\text{Sb}_y$ material system.. The energy values are in eV.

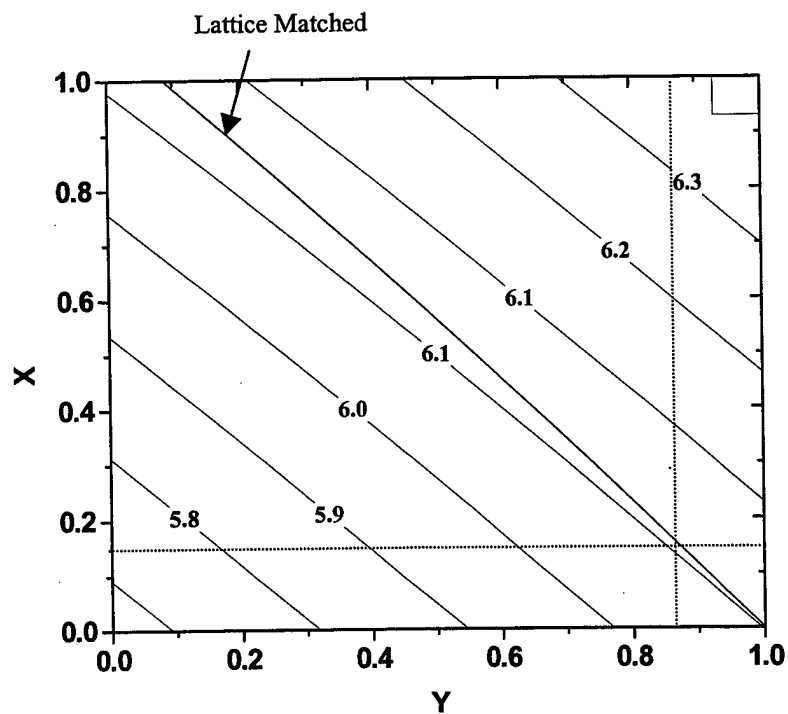


Fig. 9 Constant lattice constant contours for the $\text{In}_x\text{Ga}_{1-x}\text{As}_{1-y}\text{Sb}_y$ Material system. The lattice constant values are in Å.

Task 2.2 Design overall devices structure, including calculating the confinement factor etc.

This task was not necessary to pursue since we decided to use commercial laser bars for our laser module.

Task 2.3 Fabricate 980 nm laser bars using commercial or ASU MBE grown wafers.

We were not able to find qualified U.S. citizens at ASU to perform the MBE growths originally planned. Because of this, we decided to use commercially available laser vendors. After contacting several 980 nm laser vendors, such as Optopower, SDL, IMC Laser, etc., we decided that to use a 2 W laser from IMC Laser. Later, we acquired a 2 W laser, as well as a laser array, from Optopower.

Task 2.4 Device fabrication and characterization.

This task was not necessary to pursue since we decided to use commercial laser bars for our laser module.

IV. Summary

We have demonstrated a compact laser heatsink module that allows us to optically pump a MWIR laser with a short wavelength laser. The best result was obtained with a laser array operating at about 6 W and 10 A. This result was obtained with the laser module cooled to 77 K. The pump laser array emits at around 809 nm at room temperature. Better results could be obtained with a longer wavelength pump laser. We could also obtain better results with a properly cleaved MWIR laser.

V. Lessons Learned

By using a pulsed pump laser, such as in the Bewley paper, a very high pump power density can be achieved. With a pulsed pump laser, a pump power of 1 MW/cm^2 can be obtained because the sample heating is not a significant problem due to the small duty cycle. For example, in the Bewley paper, they used a pulse width of 107 ns with a repetition rate of 1 Hz, to give a duty cycle of $1 \times 10^{-5} \%$. With a CW pump laser, where the duty cycle is 100%, a pump power of only 1 kW/cm^2 , which is three orders of magnitude less, will have the same heat generation. We are not able to operate our pump laser at a MW/cm^2 power density and as a result we were not able to achieve lasing in our limited number of experiments.

Another problem is the absorption coefficient of the MWIR laser sample. We originally planned to grow MWIR lasers at ASU. Due to the lack of qualified students (US citizens as required by the program), we had to turn to NRL for help. The MWIR laser used in this program is not the optimum device structure to use for cw optical pumping. The biggest problem is that the active region is too thin to have significant absorption. The absorption coefficient of the MWIR active region can be estimated to be approximately $5 \times 10^3 \text{ cm}^{-1}$. Sample A has an active

region that is a 50-period InAs/GaSb/InAs/AlSb (18 Å/25 Å /18 Å /35 Å) W multiple quantum well. The total thickness is around 3050 Å (3050×10^{-8} cm). The intensity is given by

$$I = I_0 \cdot e^{-\alpha x}.$$

From this equation, I/I_0 is approximately 86%, which means that the absorption is approximately 14%, which is much too low for lasing action.

VI. Proposal for Future Work

A solution to this problem might be to use a InAs/InAs_xSb_{1-x} type-II superlattice, as reported by Zhang [3]. This type of structure can be optically pumped CW up to 95 K. This device can be modulated by a mechanical chopper at 4 kHz with a 50% duty cycle. The large duty cycle gives essentially CW operation. The advantage of using this device structure is that the absorption coefficient can be significantly increased to give a better chance at achieving lasing action.

VII. References

- [1] W.W. Bewley, *et al.*, Appl. Phys. Lett. 78, 3833 (1998). Our 3.1 μm MWIR laser is Sample A from this paper. They plot the peak output power verses pump intensity in Fig. 1 and the threshold power density verses temperature in Fig. 2 of their paper.
- [2] H.K. Choi and S.J. Eglash, Appl. Phys. Lett. 59, 1165 (1991).
- [3] Y.H.- Zhang, Appl. Phys. Lett. 66, 118 (1995).

DISTRIBUTION LIST

DTIC/OCP 8725 John J. Kingman Rd, Suite 0944 Ft Belvoir, VA 22060-6218	1 cy
AFRL/VSIL Kirtland AFB, NM 87117-5776	2 cys
AFRL/VSIIH Kirtland AFB, NM 87117-5776	1 cy
Official Record Copy AFRL/DELS/Charles Moeller	3 cys